Developmental Biology 353 (2011) 173–185

Contents lists available at ScienceDirect

Developmental Biology

journal homepage: www.elsevier.com/developmentalbiology

Assembly of RNP granules in stressed and aging oocytes requires nucleoporins and is coordinated with nuclear membrane blebbing

Joseph R. Patterson, Megan P. Wood, Jennifer A. Schisa *

Central Michigan University, Department of Biology, Mount Pleasant, MI 48859, USA

ARTICLE INFO

Article history:
Received for publication 16 December 2010
Revised 2 February 2011
Accepted 2 February 2011
Available online 5 March 2011

Keywords:
Aging
Stress
Nuclear bleb
Nucleoporin
Oocytes
Annulate lamellae

ABSTRACT

Protective cellular responses to stress and aging in the germline are essential for perpetuation of a species; however, relatively few studies have focused on how germ cells respond to stress and aging. We have previously shown that large ribonucleoprotein (RNP) complexes assemble in oocytes of *Caenorhabditis* during extended meiotic arrest or after environmental stress. Here we explore the regulation of these dynamic RNPs and demonstrate their assembly is coordinated with dramatic, nuclear membrane blebbing in oocytes. Our ultrastructural analyses reveal distinct changes in the endoplasmic reticulum, and the first evidence for the assembly of stacked annulate lamellae in *Caenorhabditis*. We further show several nucleoporins are required for the complete assembly of RNP granules, and a disruption in RNP granule assembly coupled with a low frequency of nuclear blebbing in arrested oocytes negatively impacts embryonic viability. Our observations support a model where nuclear membrane blebbing is required to increase the trafficking of nucleoporins to the cell cortex in stressed or meiotically arrested cells and to facilitate the recruitment of RNA and protein components of RNPs into large complexes. These new insights may have general implications for better understanding how germ cells preserve their integrity when fertilization is delayed and how cells respond to stress.

Introduction

Dynamic remodeling of ribonucleoproteins (RNPs) occurs as a part of normal RNA metabolism and in response to stress and aging or extended meiotic arrest (Anderson and Kedersha, 2006; Buchan et al., 2010). In all eukaryotic cells studied to date, processing bodies (P bodies) are observed which have roles in RNA degradation and storage (Parker and Sheth, 2007). Stress granules are a related but distinct RNP that are described as stalled translation initiation complexes that form in response to a variety of cellular stresses (Kedersha and Anderson, 2007). A third, related RNP granule forms in germ cells called germ granules. In the adult gonad, germ granules are proposed to function in the post-transcriptional regulation of maternal mRNAs as they emerge from nuclear pores (Pitt et al., 2000; Schisa et al., 2001; Sheth et al., 2010). In *C. elegans* germ granules are also called P granules. While P granules are perinuclear during most of development, they become dispersed in the cytoplasm of maturing oocytes and in the germline blastomeres of early embryos (Strome and Wood, 1982). Striking changes in the distribution of P granules in oocytes occur when an environmental stress is present or when ovulation is arrested (Schisa et al., 2001; Jud et al., 2008). Ovulation arrests during normal development as hermaphrodites age; at approximately 3–4 days of adulthood, when sperm become depleted, oocytes accumulate in the gonad arms with barely detectable rates of ovulation (McCarter et al., 1999). Oocytes can remain arrested in diakinesis for >5 days, which contrasts greatly with the typical ovulation rate of 23 min in young hermaphrodites. We consider this post-reproductive phase as akin to "middle-age" as it differs from the more extreme, old age when TGF-beta signaling regulates oocyte quality in 8-day-old hermaphrodites (Luo et al., 2010). Large RNP complexes assemble in stressed or arrested oocytes, containing P granules, RNA-binding proteins such as MEX-3, translationally silent mRNAs, P body proteins, and stress granule proteins (Schisa et al., 2001; Jud et al., 2008; Noble et al., 2008). The large RNP granules are enriched cortically and variably near the nuclear membrane; their structure is complex with sub-domains enriched with particular proteins. Nuclear pore complex proteins appear as distinct cytoplasmic foci that are closely associated, but adjacent to the RNP granules (Schisa et al., 2001; Jud et al., 2008). The induction of large RNP granules in response to extended meiotic arrest also occurs in the male/female nematode species *C. remanei*, and likely several other related species in which ovulation arrests in females until they mate with a male (Jud et al., 2007). The hypothesis for the function of the large RNP granules is to prevent RNA degradation or precocious translation of maternal mRNAs when fertilization is delayed.

Several recent studies link nuclear pore complex (NPC) proteins and P granules functionally. Nup98 is a mammalian nucleoporin that shuttles between the nucleus and cytoplasm and localizes on the nucleoplasmic face of NPCs (Radu et al., 1995). The worm ortholog *npp-10* associates with embryonic P granules and is required for the

* Corresponding author. Fax: +1 989 774 3462.
E-mail address: schis1j@cmich.edu (J.A. Schisa).

0012-1606/$ – see front matter © 2011 Elsevier Inc. All rights reserved.
doi:10.1016/j.ydbio.2011.02.028

integrity and function of P granules in *C. elegans* embryos (Voronina and Seydoux, 2010). Nuclear transport factors, nuclear lamin, and other nucleoporins are also implicated in regulating the localization of P granules to the nuclear membrane in early embryos (Updike and Strome, 2009; Voronina and Seydoux, 2010). In the adult gonad the perinuclear P granules of immature germ cells associate with clusters of NPCs that include mRNA export factors and interact with high levels of newly synthesized mRNA (Sheth et al., 2010). Taken together these studies suggest strong, functional associations between NPC components and P granules during normal development in the distal adult gonad and in embryos. The relationship between NPC components and P granules in the cytoplasm of *C. elegans* oocytes is currently somewhat less well understood. Interestingly, in cell culture studies, the Nup358 nucleoporin is found in the cytoplasm where it interacts with and regulates interphase microtubules (Joseph and Dasso, 2008), and in *Xenopus* extracts, Rae1 was identified as a shuttling nucleoporin that is part of a large RNP complex that controls microtubule dynamics and regulates spindle assembly (Blower et al., 2005). These, and other examples, support diverse cellular functions for NPCs in the cytoplasm (reviewed in Hetzer et al., 2005), and thus the apparent proximity of NPC components with large RNP complexes in the cytoplasm of aging oocytes is intriguing.

In this study, we wanted to gain insight into the regulation of the dynamic processes of RNP granule assembly and dissociation in stressed and arrested oocytes. We performed ultrastructural analyses to compare the fine structure of large RNP granules in oocytes with other RNPs and to examine the structure and organization of nuclear membranes and endoplasmic reticulum (ER) in stressed and arrested oocytes. In addition, we investigated the hypothesis that nucleoporins facilitate the assembly of RNP granules. We report several novel aspects of the cellular response in oocytes to stress and extended meiotic arrest: large numbers of nuclear membrane blebs form along the nuclear envelope and appear to detach; the ER reorganizes into large sheets; and assemblies of specialized nuclear membrane or ER, known as annulate lamellae, form near RNP granules at the cell cortex. Our data are consistent with a model wherein increased trafficking of nucleoporins via nuclear membrane blebbing is required for the assembly of cortical RNP granules.

Materials and methods

Strains and culture

Caenorhabditis worms were cultured as described by Brenner (1974). Strains used for this study include: N2 (Bristol) as wild type (WT); SB146, *C. remanei*; CB4108, *fog-2(q71)*; JH2184, *pie-1* prom::GFP::NPP-9::*npp-9* 3 UTR (Voronina and Seydoux, 2010). In experiments of females with arrested ovulation, females were sequestered from males at the L4 stage and allowed to grow for 1 or 3 days, post-L4. For experiments of control females with active ovulation, L4 females were added to plates with three times as many males as females, and incubated at 20 °C for 24 h. Adult females with a bulge at the vulva, indicating mating had occurred, were selected. For heat shock experiments, plates of mated females 1 day post-L4, were placed in a 34 °C incubator for 3 h before use.

Transmission electron microscopy

Adult mated, unmated and heat shocked worms were prepared according to Pitt et al. (2000). Spurr's resin was used for embedding worms and the worms were oriented for longitudinal sections. The samples were sectioned with either a Sorvall MT-2B or PowerTome X ultramicrotome. Sections were stained with uranyl acetate (saturated) for 25 min, rinsed with ddH_2O and stained with Reynold's lead citrate for 2–5 min (either 2 min for membrane resolution or 5 min for visualization of RNP granule structure) and rinsed with ddH_2O. Grids were allowed to dry and were imaged using a Phillips CM10 transmission electron microscope. Images were captured using Kodak 4489 Electron Microscope Film; negatives were developed with Kodak D19 Developer, fixed with Kodak Professional Rapid Fixer, and rinsed with Kodak Photo Flo, then digitally scanned. The images, plates, and schematic drawings were formatted and annotated using Adobe Photoshop® CS2.

Immunoelectron microscopy

Adult N2 and 3 day post L4 *fog-2* hermaphrodites were high pressure frozen and fixed in 2% paraformaldehyde, 0.5% glutaraldehyde, 0.1% uranyl acetate, and 2% H_2O in methanol, as described in Hall et al. (in press). Immunogold labeling was performed according to Paupard et al. (2001). Grids were fixed in 5% glutaraldehyde for 5 min, washed with H_2O, stained with 5% UA and imaged using a Phillips CM10 TEM. Gold labeling distribution and density was calculated using the micrograph method for gold density over a profile area (Lucocq, 2008). Images and plates were formatted using Adobe Photoshop® CS2.

Fluorescence microscopy and time-lapse imaging

Antibodies and staining protocols were as described: MEX-3 (Draper et al., 1996) (antibody from Dr. James Priess), and mAb414 that detects several nuclear pore proteins (BABCO; Pitt et al., 2000). Secondary antibodies were used at a 1:200 dilution (Molecular Probes). Samples were imaged using a Nikon A1R laser scanning confocal system or an Olympus Fluoview 300 laser scanning confocal microscope. The images were compiled and formatted using Adobe Photoshop® CS2.

Time-lapse imaging of GFP::NPP-9 was performed using a Nikon A1R laser scanning confocal system. Worms were anesthetized in M9 buffer containing 0.01% levamisole and 0.1% tricaine for 30 min prior to imaging (McCarter et al., 1999). A Tokai Hit stage top incubator was used to control the temperature at 34 °C.

RNAi

A large number of gravid *fog-2(q71)* hermaphrodites were grown on NGM plates. Adult worms were bleached to synchronize the population. Newly hatched L1 worms were pipetted onto RNAi plates containing carbenicillin and IPTG (Kamath and Ahringer, 2003). In parallel, bacteria were streaked from glycerol stocks onto LB plates with carbenicillin and incubated at 37 °C for 24 h. A single colony was picked from the plate and grown in Luria broth (LB) and carbenicillin at 37 °C for 6–12 h. The clone for *inx-14* served as a positive control. The empty vector L4440 was the negative control. A 300 μL aliquot of each bacterial culture from the Ahringer RNAi library was pipetted onto each of 5 RNAi plates. The plates were allowed to dry and incubated at 24 °C overnight. The L1 worms were rinsed in dH_20 and then approximately 60 L1 worms were transferred to 3 of 5 seeded plates using a mouth pipette. The worms were incubated at 24 °C for approximately 26 h, or until the worms reached the L4 stage. L4 females were moved to the 2 remaining seeded RNAi plates. The female worms were grown at 24 °C for approximately 24 h in order for the oocytes to accumulate in the proximal gonad arms. The gonads were dissected and the worms were fixed and stained for MEX-3 as described (Jud et al., 2008; Draper et al., 1996). Samples were imaged using a Nikon A1R laser scanning confocal microscope.

Oocyte viability analysis

To determine the viability of arrested oocytes after RNAi of *kgb-1* in the GFP::MEX-3; *fog-2(q71)* strain, methods were essentially as described in Jud et al. (2007). The number of oocytes accumulated in the gonad arm was counted, and GFP distribution was scored as large

granules, cytoplasmic, or intermediate. Matings were set with individual females and *fog-2(q71)* males. The time needed for the accumulated oocytes to be fertilized and laid was determined empirically, by checking the plates frequently and counting the total number of unfertilized oocytes, embryos, and larvae on the plate. When that number was equal to the number of oocytes accumulated prior to mating, adults were removed from the plates so no additional embryos or oocytes could be laid. Viability of embryos was scored 24 h later, by counting numbers of hatched larvae vs. unhatched embryos.

Results

Detection of novel nuclear membrane blebs in arrested oocytes

Given the apparent close proximity of nucleoporins with large RNPs in aging oocytes (Pitt et al., 2000; Jud et al., 2007), we decided to first more closely analyze this relationship by examining rotations of confocal slices of co-stained *C. elegans* germlines. MEX-3 is one of several putative RNA-binding proteins that localizes to large RNPs in aging oocytes (Schisa et al., 2001). We confirmed that while not all cytoplasmic foci of nucleoporins are adjacent to MEX-3 granules, 90% of large MEX-3 granules (greater than or equal to 1.0 μm in diameter) are within 0.5 μm of nuclear pore protein foci; the smaller nuclear pore protein foci often appear to be "docked" on the larger MEX-3 granules (Fig. 1). The distribution of both MEX-3 and nuclear pore protein granules showed reproducible enrichment near the plasma membrane, and though we did not quantitatively define the cortex region of the cytoplasm, we refer to this granule localization near the plasma membrane as cortical.

We next set out to examine the ultrastructure of arrested oocytes in *C. elegans* and *C. remanei*. We first focused on unmated *C. remanei* females because in this male/female species delays in the fertilization of oocytes occur as part of normal development in young females prior to the generation of any progeny. This contrasts with the hermaphroditic species *C. elegans* in which oocytes are fertilized every 23 min in young worms, and approximately 300 progeny are generated before sperm are depleted (McCarter et al., 1999). We have speculated that the presence of large RNPs in arrested oocytes of middle-aged *C. elegans* is due to conservation from an ancestral gonochoristic (male/female) state (Jud et al., 2007; Kiontke and Fitch, 2005); thus, it seems appropriate to study meiotically arrested oocytes in a male/female species. In addition, arrested oocytes in *C. elegans* are found only in middle-aged hermaphrodites depleted of sperm or in genetic mutants such as *fog-2* in which no sperm are ever produced; therefore, indirect effects of somatic aging or the genetic background can potentially complicate germline studies. In arrested *C. remanei* oocytes, we noticed unusual "bubble-like structures" along the nuclear membrane that we refer to as nuclear membrane blebs. The size of the nuclear blebs ranged from 730 to 210 nm in diameter (average = 460 ± 150 nm; Fig. 2A; Table 1). Higher magnification images revealed multiple bilayer membranes instead of the typical, single bilayer nuclear membrane (Fig. 2B and C). In 92% of oocytes, we saw clear views of regions with multiple membranes, with an average of 4.3 blebs per oocyte (Table 1). Nuclear pores were evident in many of the membranes (Fig. 2C). P granules were sometimes seen along the nuclear membrane adjacent to the region of nuclear blebs (Fig. 2B, arrow). In the majority of control oocytes from mated females (70%), the nuclear membrane was continuous, lacking any regions of membrane blebbing (data not shown). In the minority of mated females, an average of 1.1 blebs per oocyte was observed (Table 1); the blebs were generally much smaller than those in oocytes of unmated females (Fig. 2D); the maximum diameter observed was 210 nm (average = 160 ± 40 nm). In other cell types, including the immature germ cells located distal of the oocytes, and somatic sheath cells, the nuclear membrane appeared continuous without obvious evidence of nuclear blebs (data not shown). Therefore, our data suggest that nuclear membrane blebs form in oocytes, and their frequency and size increases when oocytes are arrested in unmated females (Supplementary Table 1).

Our ultrastructural analysis was based on a limited number of random, not serial, thin sections through gonads; thus, in order to better ascertain the distribution and frequency of nuclear blebs in oocytes, we performed immunostaining for nuclear pore proteins. We used the monoclonal antibody 414 (mAb414) that recognizes multiple nuclear pore proteins in *Caenorhabditis* (Aris and Blobel, 1989; Browning and Strome, 1996; Jud et al., 2007) and found the nuclear blebs were visible at high magnification by light microscopy. We quantitated blebs along the nuclear envelope and defined nuclear blebs as membranes that appeared in cross-section as ovals or circles surrounding a non-fluorescent center. In unmated females, 100% of the oocytes had obvious nuclear blebs, with an average of 3.5 blebs per oocyte (Table 1). The blebs varied considerably in appearance; one of the largest blebs measured 5.1 μm in diameter (average = 1140 ± 1140 nm; Fig. 3A). In other oocytes, pairs of blebs were in close proximity to one another (Fig. 3B and C, double arrows); less frequently, up to four discrete blebs were clustered (Fig. 3C and inset) that may correspond to the four bilayer membranes seen by TEM in thin sections (Fig. 2B and C). In oocytes of mated females, nuclear blebs were detected in 31% of oocytes (Table 1; Fig. 3D–F), with an average of 0.4 blebs per oocyte.

In the mAb414-stained oocytes of unmated females, multiple cytoplasmic foci were seen in addition to the prominent staining on the nuclear envelope. We observed blebs that extended into the cytoplasm (Fig. 4A), C-shaped cross-sections of blebs, and cross sections of spherical blebs that were in close proximity, but not attached, to the nuclear envelope (Fig. 4B and C). We also asked if detached blebs were visible in our TEM images. In thin sections of arrested oocytes, we observed regions of the nuclear membrane with multiple bilayer membranes (Fig. 5A). In other oocytes nuclear blebs appeared to be in the process of detaching or detached from the nuclear membrane (Fig. 5B and C). The blebs contained material similar in electron density to the nucleoplasm. A subset of blebs did

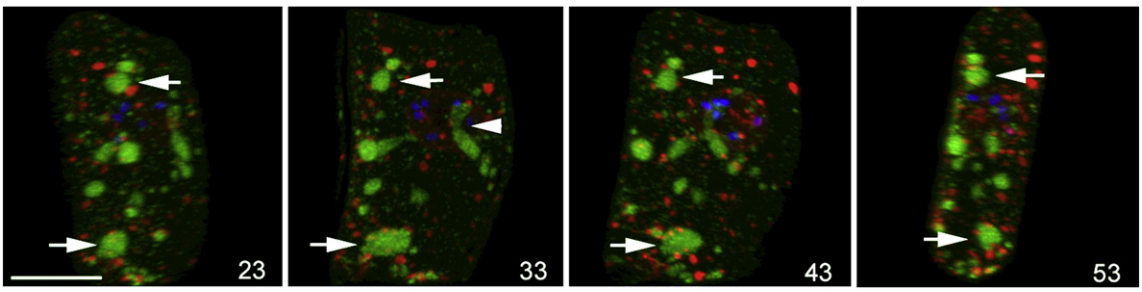

Fig. 1. Assembly of ribonucleoprotein granules in arrested oocytes. Confocal rotation series of a single oocyte from a *fog-2* unmated female. Foci of nuclear pore proteins (red) are abundant in the cytoplasm and cortex and sometimes appear to dock on larger RNP granules that include MEX-3 (green), arrows. Many granules appear spherical, while some are irregularly shaped, small arrowhead in frame 33. DNA is stained with DAPI (blue). Scale bar: 10 μm.

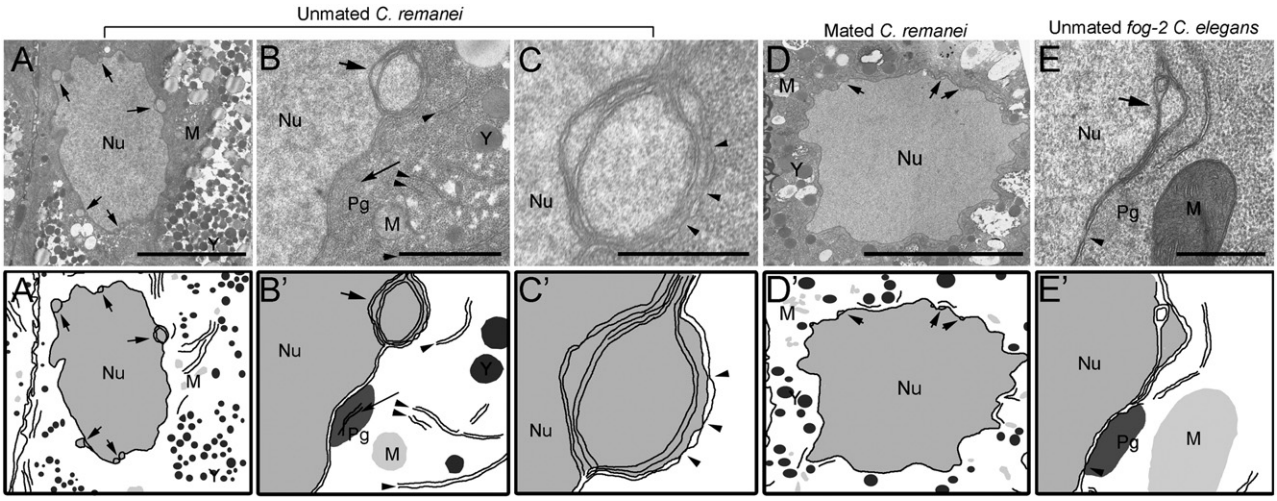

Fig. 2. Ultrastructure of nuclear blebs composed of multiple nuclear membranes in arrested oocytes. (A–C) Nuclear blebs are evident in thin sections of an arrested oocyte of an unmated *C. remanei* female. (A′–C′) Schematic drawings. (A) Arrows indicate 5 distinct nuclear blebs along the nuclear membrane of the nucleus (Nu). Abundant yolk particles (Y) are visible. Scale bar: 5 μm. (B) High magnification view of a single nuclear bleb; membranes of the endoplasmic reticulum (arrowheads), mitochondria (M), and membranes containing nuclear pores (arrows) are in proximity to the nuclear bleb. P granules (Pg) are sometimes observed near the nuclear blebs. Scale bar: 1 μm. (C) High magnification view of nuclear bleb reveals 4 double membranes and distinct nuclear pores in at least the most cytoplasmic membrane (arrowheads). Scale bar: 0.5 μm. (D) Oocytes in mated *C. remanei* females have a generally continuous bilayer nuclear membrane; occasional small nuclear blebs can be seen (arrows). Scale bar: 5 μm. (E) Nuclear blebs are detected in arrested oocytes of unmated *fog-2 C. elegans* females (arrow). P granules (Pg) are sometimes observed near the nuclear blebs. Scale bar: 0.5 μm. (D′–E′) Schematic drawings.

not appear to be continuous with the nuclear membrane although in random thin sections, we could not be certain they were completely detached from the nucleus. Since increased numbers of nuclear pore protein foci are detected in the cytoplasm of arrested oocytes in unmated females (Jud et al., 2007), blebbing of the nuclear membrane might represent a mechanism for trafficking portions of the nuclear membrane between the nucleus and the cytoplasm.

Heat shock induces nuclear membrane blebs in oocytes

Several cytological changes in arrested oocytes have also been observed in environmentally stressed oocytes. In the nucleus, chromosomes associate with the nuclear periphery after exposure to anoxia or when ovulation is arrested (Hajeri et al., 2010). In the cytoplasm, heat shock, osmotic stress, and anoxia are each sufficient to induce a dramatic relocalization of MEX-3 protein into large RNP granules, similar to the RNP granules seen in arrested oocytes (Jud et al., 2008). Therefore, we next asked if the nuclear membrane blebs discovered in arrested oocytes were similarly induced by heat shock. In thin sections nuclear blebs were observed along the nuclear membrane in 70% of heat-shocked *C. remanei* oocytes, just as in arrested oocytes; however, the density of nuclear blebs appeared lower than in arrested oocytes (Table 1). To better quantify the extent of nuclear blebs throughout heat shocked oocytes, we performed fluorescence microscopy using the mAb414 antibody. Analyses of confocal sections revealed an average of 3.1 nuclear blebs along the nuclear envelope per oocyte (Table 1). Nuclear blebs were seen within the nuclear membrane, as well as in close proximity to, but detached from the nuclear membrane (Fig. 4D–F). The distribution and diameter of the heat shock-induced blebs were similar to the ranges seen in arrested oocytes (Table 1). Taken together, the data indicate that heat shock induces an increased frequency of nuclear blebs in oocytes, similar to that observed in arrested oocytes (Supplementary Table 1).

Nuclear membrane blebs may traffic nucleoporins to annulate lamellae in the cell cortex

The trafficking or shuttling of nucleoporins is well documented (Hetzer et al., 2005), and in many species and cell types, stacks of nuclear pore-containing membranes assemble in the cytoplasm called annulate lamellae (Kessel, 1989). Having observed nuclear blebs in the cytoplasm that appeared to be trafficking nuclear membrane to or from the cell cortex, we next asked if we could find evidence of annulate lamellae in *Caenorhabditis* by TEM. Stacks of membrane were detected in 42% of arrested oocytes of unmated *C. remanei* females (Fig. 6A–D). The membranes were sometimes along the periphery of electron dense granules (Fig. 6A) and sometimes appeared embedded within the granules (Fig. 6C). In higher magnification images unambiguous nuclear pore complexes were seen in the membranes; moreover, several pores were aligned within the membrane relative to neighboring membranes (Fig. 6B and D). These stacks of nuclear pore-containing membranes appeared very similar to the annulate lamellae reported in the arrested oocytes of several species including

Table 1
Nuclear blebs in oocytes increase in frequency and size during extended meiotic arrest or heat-stress.

	TEM			Confocal		
	Frequency (% oocytes with blebs)	Frequency (# blebs per oocyte)	Avg. diameter of bleb (nm)	Frequency (% oocytes with blebs)	Frequency (# blebs per oocyte)	Avg. diameter of bleb (nm)
Mated *C. remanei*	30 ($n=10$)	1.1	160±40	31 ($n=29$)	0.4	540±220
Unmated *C. remanei*	92 ($n=12$)	4.3	460±150	100 ($n=30$)	3.5	1140±1140
Heat Shocked *C. remanei*	70 ($n=10$)	2.7	360±190	100 ($n=41$)	3.1	950±540
Mated *C. elegans*	ND	ND	ND	33 ($n=33$)	0.4	830±540
Unmated *fog-2 C. elegans*	ND	ND	ND	100 ($n=34$)	3.7	1210±610
Heat shocked unmated *fog-2 C. elegans*	ND	ND	ND	100 (33)	5.6	1840±880

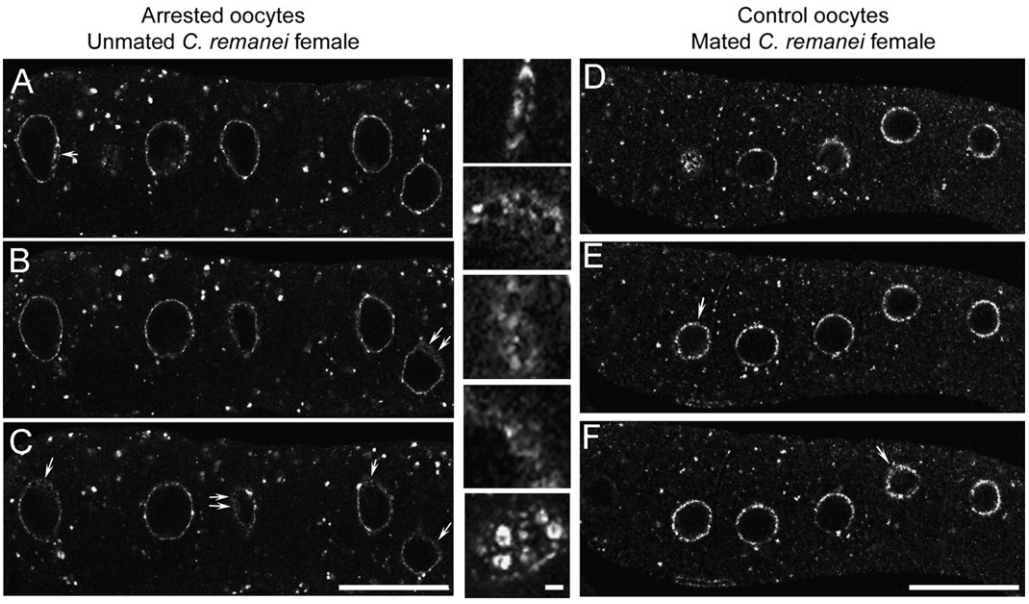

Fig. 3. Nuclear blebs are more abundant in arrested oocytes of unmated worms than in actively ovulated oocytes of mated worms. (A–F) Single confocal slices of oocytes in which nuclear membranes were detected with mAb414. (A–C) Numerous nuclear blebs are seen in multiple *z*-sections of a row of arrested oocytes in an unmated female (arrows). Scale bars: 20 μm. Insets show higher magnification of variety of forms of nuclear blebs. Scale bar: 1 μm. (D–F) Fewer nuclear blebs (arrows) are detected in *z*-sections of a row of actively ovulated oocytes in a mated female. Scale bars: 20 μm.

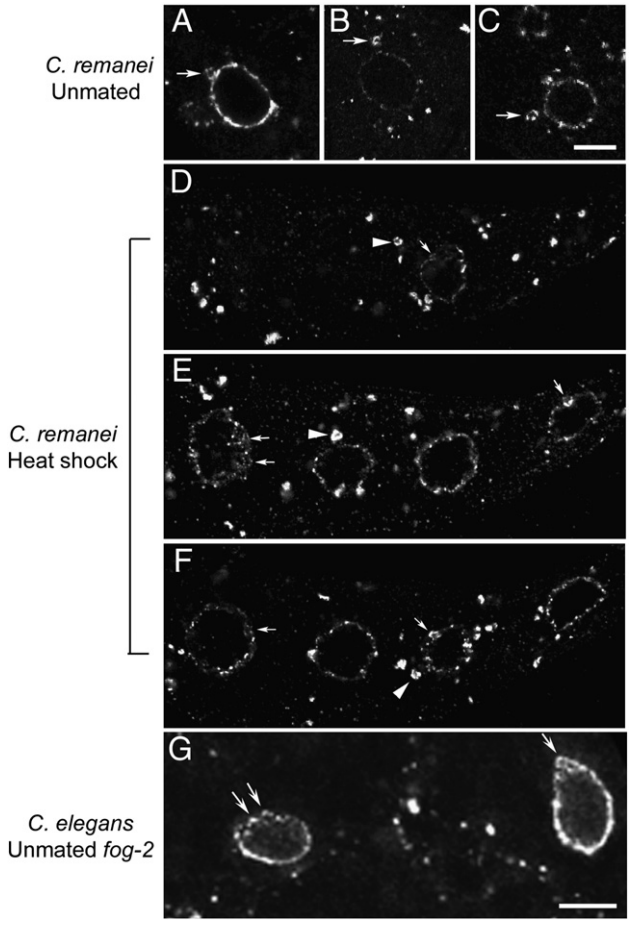

Fig. 4. Nuclear blebs appear to detach from the nucleus and can be induced by heat shock. (A–C) Nuclear blebs that appear to be detaching (A) or have detached (B–C) from the nuclear membrane (detected with mAb414) in arrested *C. remanei* oocytes (arrows). (D–F) Nuclear blebs occur at high frequency after heat shock of mated females. Detached blebs (arrow head) and nuclear blebs on the nuclear membrane (arrows) are evident in multiple *z*-sections of a row of oocytes. (G) Nuclear blebs also occur in arrested *C. elegans* oocytes of unmated *fog-2* worms (arrows). Scale bars: 10 μm.

Xenopus (Kessel, 1989). To our knowledge this is the first evidence for the assembly of large stacks of annulate lamellae in nematodes, though they may be related to the single membranes with nuclear pore-like features shown by Pitt et al. (2000).

To determine if heat shock also induces the formation of annulate lamellae in oocytes, we examined thin sections of heat-shocked, mated females. In 20% of oocytes we detected annulate lamellae near RNP granules in close proximity to the plasma membrane (Fig. 6E and F). While the nuclear pores were sometimes difficult to confirm due to the electron dense regions of the granules seen beneath all annulate lamellae observed ($n=6$ including thin sections of both arrested and heat shocked oocytes), the largest assembly impressively included eleven aligned membranes.

Nucleoporin trafficking in oocytes is conserved in C. elegans

In examining the ultrastructure of nuclear blebs in arrested oocytes, we noted that some of the nuclear blebs were adjacent to the region of nuclear membrane directly below a P granule (Fig. 2B). Because we were not aware of any antibodies that recognize P granules in *C. remanei*, but had antibodies for P granule proteins in *C. elegans*, we conducted a co-staining experiment for PGL-1 and mAb414 with the *C. elegans fog-2* strain. The phenotype of hermaphrodites in this mutant strain mimics females in *C. remanei*; no sperm are produced; thus, the unmated *fog-2* hermaphrodite is often referred to as a female (Schedl and Kimble, 1988). The results did not support a close relationship between nuclear membrane blebs and P granules in oocytes along the nuclear envelope (data not shown); however, we were able to confirm that nuclear membrane blebs occur in *C. elegans* oocytes, and they increase in frequency when ovulation is arrested (Fig. 4G; Table 1). We also noted a close association between nuclear pore proteins and PGL-1 near the nuclear membrane, indicating that newly detached nuclear membrane blebs are closely associated with P granules (data not shown). Using TEM as a complementary technique, nuclear membrane blebs were detected in oocytes of *fog-2* unmated females that resembled those observed in *C. remanei* (Fig. 2E). We next asked whether stacks of annulate lamellae could be detected in the cortex of *C. elegans fog-2* arrested oocytes and found evidence of annulate lamellae in 10.5% of oocytes (Fig. 6G and H). Though the

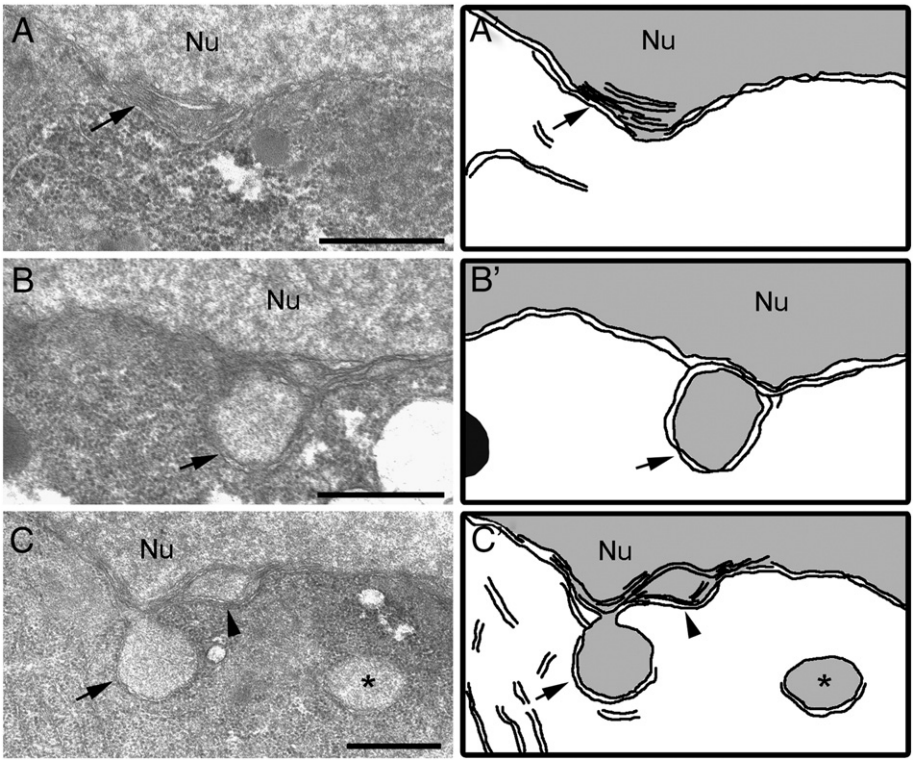

Fig. 5. Ultrastructure of detached nuclear blebs in arrested oocytes. (A–C) Thin sections of arrested oocytes in unmated *C. remanei* females. (A′–C′) Schematic drawings. (A) Multiple membranes accumulate along the nuclear membrane (arrow). (B) A nuclear bleb is extended into the cytoplasm and is composed of multiple nuclear membranes. (C) A nuclear bleb appears to be nearly detached (arrow); a second nuclear bleb appears to be forming within the nuclear membrane (arrowhead); and a third bleb appears to be completely detached from the nucleus (asterisk). Scale bars: 5 μm.

number of thin sections showing annulate lamellae was limited ($n=3$), in all cases, the lamellae were associated with RNP granules. Thus, all of the cellular responses discovered in *C. remanei* are also apparent in stressed or arrested *C. elegans* oocytes (Supplementary Table 1).

Insights into the ultrastructure of cortical RNP granules

One of our original goals was to characterize the fine structure of RNP granules in arrested and stressed oocytes. A variety of RNP granule morphologies were observed in arrested oocytes of both *C. remanei* and *C. elegans* (Fig. 7; data not shown) that were not seen in oocytes of control, mated females. The granules varied in electron density, size and shape, subcellular location, proximity to mitochondria, and association to membranes. However all granules were easily distinguished from the prominent yolk particles (Fig. 7A) and none were delineated by a membrane. Most granules were cortically localized, in close proximity to the plasma membrane (Fig. 7), while some were located adjacent to the nuclear envelope (data not shown). These locations correlate with their appearance in fluorescence microscopy (Jud et al., 2007, 2008). A subset of granules was associated with one or more bilayer membranes (Fig. 6), and the granules ranged from 200 nm to 3 μm in diameter. Some small granules were fairly compact and electron dense; however, others had irregular outlines in cross-section and were of moderate electron density (Fig. 7; data not shown). The irregular outlines of many granules may be indicative of remodeling of the RNPs, which has been observed for stress granules (Kedersha et al., 2005; Souquere et al., 2009).

The ultrastructure of heat shock-induced stress granules differs from that of granules induced by alternative stresses (Souquere et al., 2009). To better define the oocyte RNP granules in relation to stress granules, we next asked if the ultrastructure of RNP granules induced by heat shock was similar to that of the RNP granules induced by arrested ovulation. The heat shock-induced RNPs were generally cortically localized, similar to those seen in arrested oocytes. They varied in size, from 883 nm to 2.5 μm in diameter. The heat shock-induced RNPs also varied somewhat in their ultrastructural characteristics; in some granules, regions of heterogeneous electron density were evident (data not shown), similar to the heterogeneity in a subset of RNPs in arrested oocytes (Fig. 7B).

The positive identification of oocyte RNP granules in thin sections was complicated by the presence of P granules and P bodies, two types of smaller RNPs localized throughout the germline cytoplasm irrespective of stress, or the presence of sperm and ovulation rate. To describe the larger cortical granules seen in the thin sections, we initially relied on size and subcellular location which were consistent with the RNP granules previously studied by fluorescence microscopy (Jud et al., 2007; Jud et al., 2008). To verify their identity, however, we turned to immunogold labeling of *C. elegans* arrested oocytes, using high pressure freezing fixation to balance preservation of morphology with permeability for the antibodies. CGH-1 primary antibody, the worm ortholog of the P body and stress granule protein RCK/p54 (Kedersha and Anderson, 2007), positively recognizes RNP granules in arrested and heat-shocked oocytes (Jud et al., 2008); it was identified by TEM using gold-labeled secondary antibody. In arrested oocytes of unmated *fog-2* females, the CGH-1 immunoreactivity was at highest concentrations clustered within large, electron dense granules at the oocyte cortex (Fig. 8A and B); 87% of gold particles contacted RNP granules ($n=2660$ gold particles). The average density of gold particles on granules was 133/μm^2, in contrast to 1.7/μm^2 in areas not including granules. In the control oocytes of mated females, immunoreactivity was dispersed or in small clusters, as expected for the distribution of CGH-1 in these oocytes (Navarro et al., 2001; data not shown). In confocal analyses, CGH-1 co-localizes with MEX-3 and

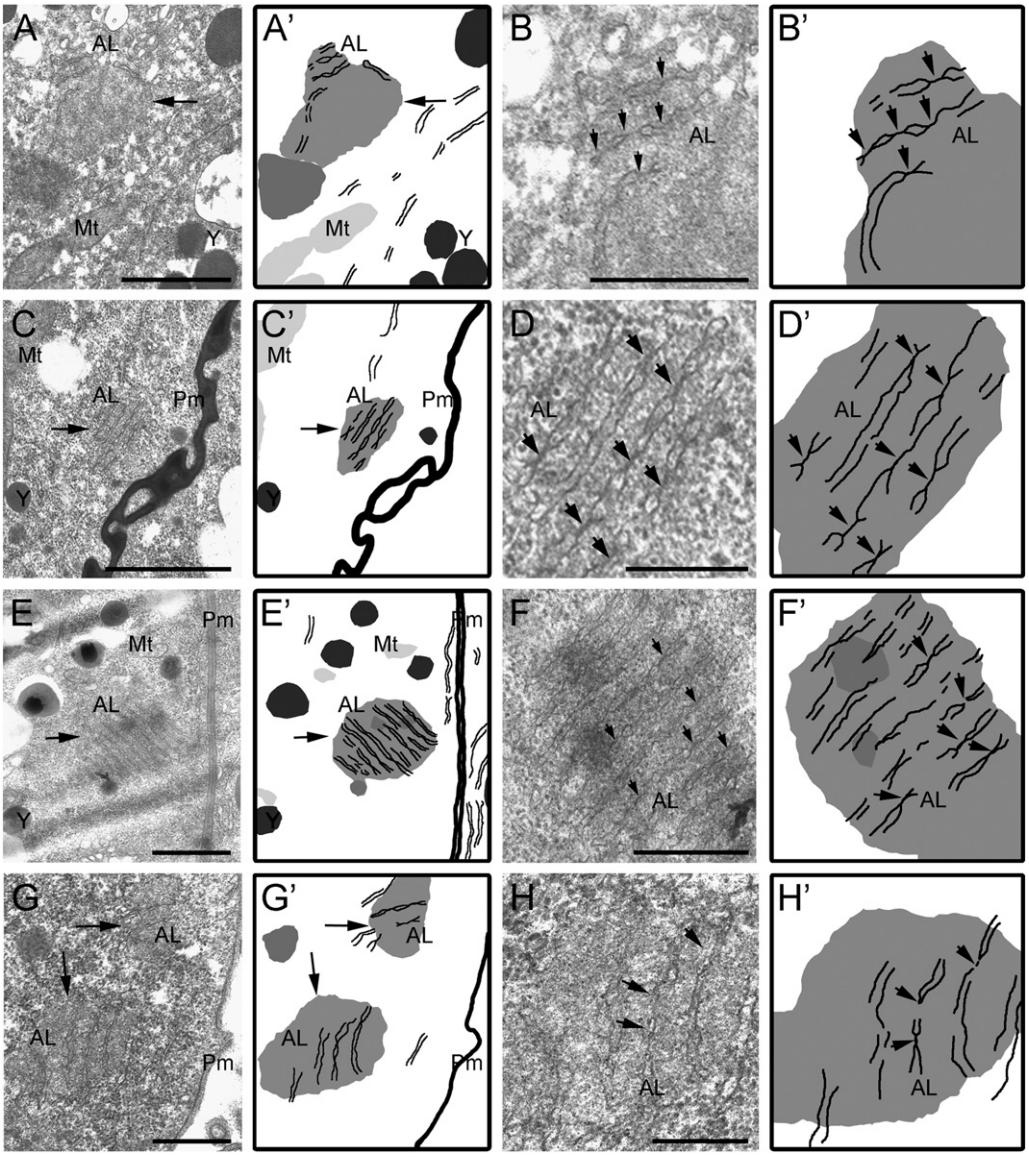

Fig. 6. Annulate lamellae appear in close proximity to cortical RNP granules. (A–D) Thin sections of arrested oocytes in unmated *C. remanei* females. (A) Annulate lamellae (AL) adjacent to an RNP granule (arrow). Scale bar: 1 μm. (B) High magnification view of annulate lamellae in A, resolves nuclear pores in aligned membranes (arrows). Scale bar: 0.5 μm. (C) Micrograph of AL in close proximity to, or contacting a cortical RNP granule near the plasma membrane (Pm). Scale bar: 1 μm. (D) High magnification view of AL in C shows distinct nuclear pores in aligned membranes (arrows). Scale bar: 0.25 μm. (E–F) Thin sections of oocytes after heat shock of mated *C. remanei* females. (E) Annulate lamellae cortically located and in close association to an RNP granule (arrow) Scale bar: 1 μm. (F) High magnification view of AL in E shows nuclear pores in membranes (arrows). Scale bar: 0.5 μm. (G–H) Thin sections of arrested oocytes in unmated *C. elegans fog-2* females. (G) Two cortical RNP granules appear to contact AL (arrows). Scale bar: 1 μm. (H) High magnification view of AL in G shows nuclear pores in membranes (arrows). (A′–H′) Schematic drawings. Scale bar: 0.5 μm.

other RNA-binding proteins in RNP granules of arrested oocytes (Jud et al., 2008); in contrast, the nuclear pore proteins detected with mAb414 appear to be closely associated, but not co-localized with the large RNP granules (Fig. 1). To further characterize the relationship between the nuclear pore proteins and RNP granules, immuno-EM was performed to simultaneously visualize CGH-1 and nuclear pore proteins. In the control mAb414-stained sections, mesh-like structures in the cortex were covered with gold that were consistent with the annulate lamellae seen previously (Figs. 6 and 8C, D). The lighter fixation and staining conditions necessary for immuno-EM do not allow good visualization of membranes; therefore, direct comparisons are difficult. In the co-stained sections, multiple examples of large RNP granules covered with 12 nm gold (CGH-1) were adjacent to smaller mesh-like structures covered with 6 nm gold (nuclear pore proteins) (Fig. 8E and F). The few 12 nm particles seen in the presumptive annulate lamellae were only at the periphery, confirming that CGH-1 is closely associated, but not co-localized to a large extent, with nuclear pore proteins.

Model of coordinated cellular response to stress and aging in oocytes

Our results demonstrate that stress and aging can each elicit a coordinated cellular response in oocytes including increased nuclear membrane blebbing and assembly of RNP granules. We also observed that the responses to stress and aging appear very similar in *C. elegans* and *C. remanei* oocytes (Supplemental Table 1). We asked if the effects of stress and aging were additive on the extent or size of nuclear blebbing, as they are for the size of RNP granules (Jud et al., 2008); we found that in heat-shocked, unmated *C. elegans fog-2* females, the average nuclear bleb diameter was 1.84 μm and the frequency was 5.6 blebs per oocyte, both higher than with either stress or arrest alone (Table 1). The coincidental detection of nuclear blebs, annulate

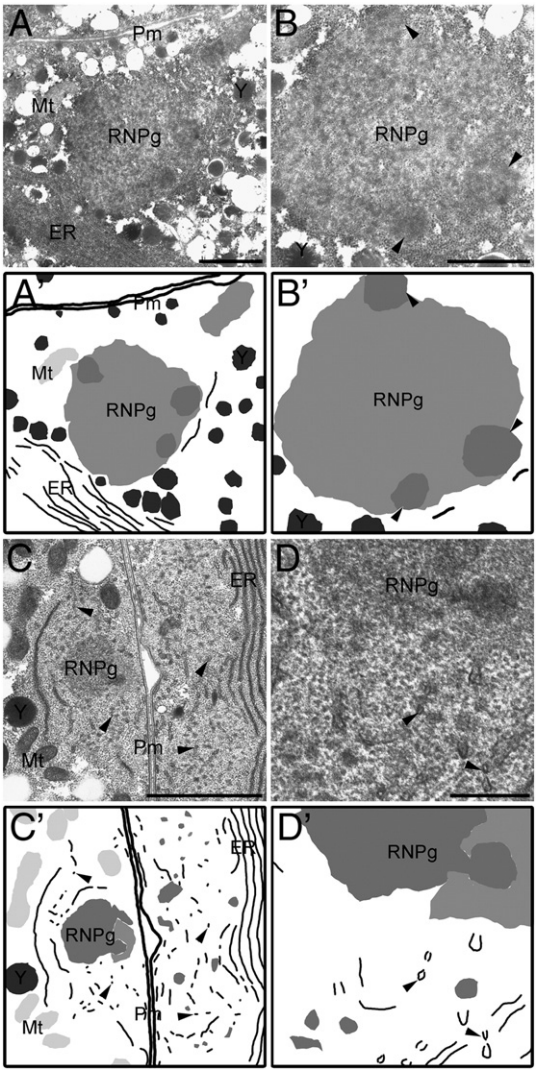

Fig. 7. Ultrastructure of large RNP granules reveals heterogeneous substructure. (A) In a thin section of a *C. remanei* arrested oocyte, a cortically located RNP granule, RNPg, is located near large sheets of endoplasmic reticulum (ER) mitochondria (Mt) Yolk (Y) and the plasma membrane (Pm). Scale bar: 1 μm. (B) High magnification view of the RNP granule in (A) reveals highly electron dense patches within the granular area (arrowheads). Scale bar: 1 μm. (C) Thin section of a *C. remanei* mated female after heat shock shows a cortically located RNP granule. Large sheets of ER are evident in adjacent oocyte and in cross-section in both oocytes (arrowheads). Scale bar: 1 μm. (D) High magnification view of the RNP granule in C. (A′–D′) Schematic drawings. Scale bar: 0.5 μm.

lamellae, and RNP granules suggests a functional relationship among these three structures. One model consistent with our data proposes the increased trafficking of nucleoporins to the cell cortex via nuclear blebs facilitates the assembly of RNP granules (Fig. 9). To establish a better understanding of the temporal sequence of cellular responses in oocytes, we decided to quantitate nuclear blebs in proximal and more distal oocytes of young *fog-2* females. The oocytes in these females do not immediately assemble RNP granules; the first MEX-3 granules are seen in the most proximal oocytes between 6 and 8 h into adulthood, but MEX-3 remains cytoplasmic in the more distal oocytes at this transitional developmental stage (Jud et al., 2008; Megan Wood, unpublished data). We asked how many nuclear blebs were visible in the proximal oocytes that contained RNP granules, and in the more distal oocytes lacking RNP granules. We found that the frequency of nuclear blebs in distal oocytes, where MEX-3 had not yet assembled into granules, was increased relative to that in oocytes of mated N2 hermaphrodites (Fig. 10). This finding was consistent with our model that nuclear blebs occur in oocytes prior to the assembly of detectable, large RNP granules.

Our model further implies that disruption of nucleoporin trafficking could interfere with RNP granule assembly. As a first test of this prediction, we used RNAi to down-regulate the expression of nuclear lamin, and selected nucleoporins, and nuclear transport factors. We found that *npp-9*, *npp-10*, *ran-4*, *ran-1*, *xpo-1*, and *lmn-1* were required at variable penetrance, for assembly of MEX-3 into large RNP granules in arrested oocytes (Fig. 11; Supplemental Table 2; data not shown). The penetrance was <10% for complete failure of MEX-3 granules to assemble after RNAi of *ran-1* and *xpo-1*; however, the great majority of worms assembled smaller granules than controls (Supplemental Table 2; Fig. 11). Explanations for these results include the possibility that ovulation resumed in the *fog-2* females after RNAi; however, we did not observe unfertilized oocytes in the uterus of these worms. Additional interpretations of the failure of MEX-3 to assemble into large granules are further considered in the discussion. We conclude that our results are consistent with a model in which nucleoporin trafficking is required for assembly of large cortical RNP granules in arrested oocytes.

A second important question related to our model is the consequence to the worm if nuclear blebbing and/or RNP granule assembly are not induced in meiotically arrested oocytes. In an ongoing RNAi screen in the lab, we identified a member of the Jun-N-terminal kinase (JNK) subfamily of MAP kinases, *kgb-1*, as a positive regulator of RNP granule assembly at low penetrance (J. Schisa, unpublished results). We determined that the number of nuclear blebs/oocyte in *fog-2*; *kgb-1(RNAi)* females was reduced, 0.7 blebs/oocyte ($n=32$), compared to *fog-2* females, 3.7 blebs/oocyte ($n=34$). We therefore next asked if the meiotically arrested oocytes lacking nuclear blebs and RNP granules gave rise to viable offspring. We mated males with GFP::MEX-3;*fog-2;kgb-1(RNAi)* females and asked how many of the arrested oocytes with cytoplasmic GFP::MEX-3 eventually gave rise to viable larvae. We found that viability decreased from 92.8% when GFP::MEX-3 granules had assembled in oocytes, to 72.9% when GFP::MEX-3 granules failed to assemble. Thus, these results provide evidence that an increased frequency of nuclear blebbing and coordinated assembly of RNP granules play a protective role when oocytes are delayed in being fertilized. Consequences of arrested oocytes failing to increase nuclear blebbing or assemble RNP granules appear to include increased risk of embryonic lethality. Future experiments should determine the biochemical function of KGB-1 in these cellular responses and characterize additional regulators of RNP granule assembly to continue testing the hypothesis for the biological function of RNP granules.

Discussion

In this work, we discovered that stress and extended meiotic arrest elicit the formation of nuclear membrane blebs that form concomitantly with cortical RNP granules in oocytes. The nuclear membrane blebs appear to detach into the cytoplasm where they may transit to the cell cortex; thus, it seems likely they are a transition state for shuttling of nucleoporins. We also show, for the first time in nematodes, that annulate lamellae assemble in the cortex of arrested and stressed oocytes (Fig. 6), and provide evidence consistent with nucleoporin trafficking being functionally linked with the assembly of large, cortical RNP granules. We further characterize changes in the ultrastructure of arrested and stressed oocytes, including the assembly of large RNP granules. Taken together, these data suggest that both environmental stress and quiescence, or extended meiotic arrest, can induce a complex series of cellular responses in oocytes that are dynamic and reversible. The similarities of the responses to such different stimuli suggest these responses may have a fundamental function such as protecting oocytes when fertilization is delayed. Indeed our results with *kgb-1* are the first to directly link

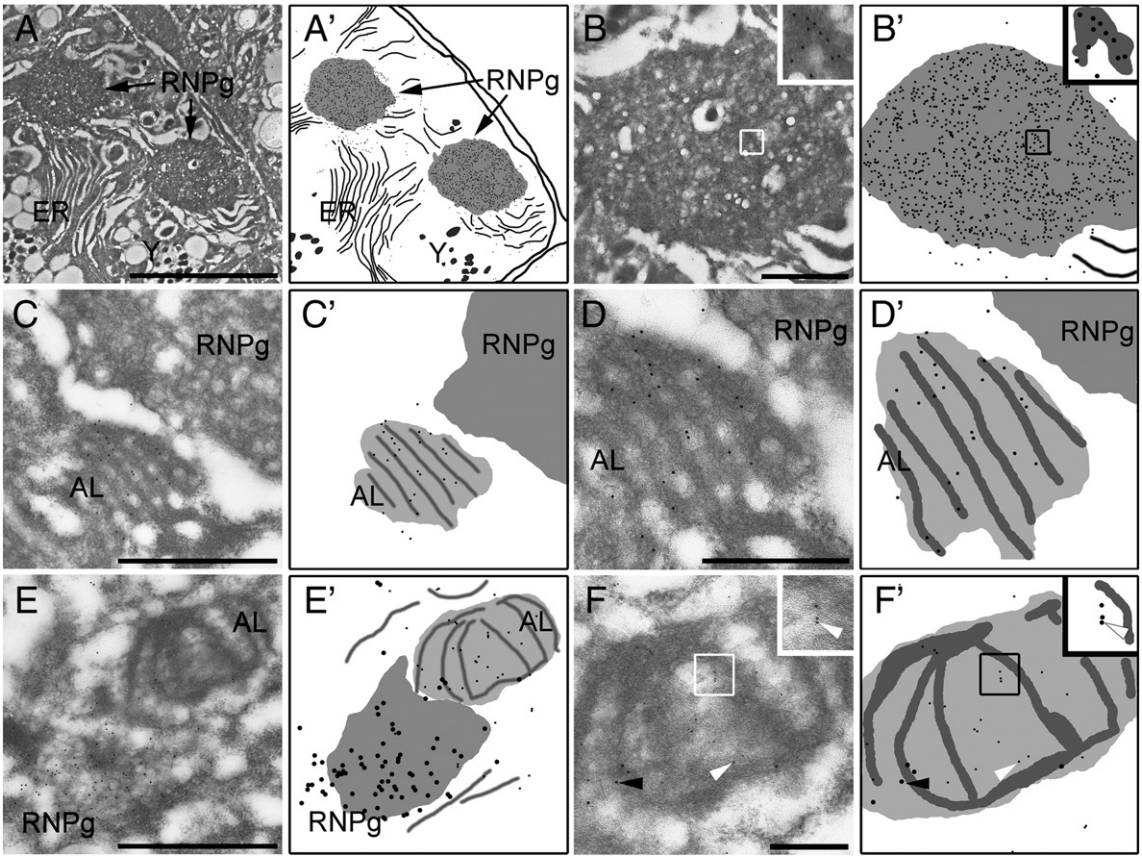

Fig. 8. Accumulation of CGH-1 in RNP granules of arrested *fog-2* oocytes and in close proximity to nuclear pore proteins. (A–B) RNP granules, RNPg, labeled for the granule component CGH-1 with 12 nm gold particles. (A′–B′) Schematic drawings. (A) Two RNP granules are located cortically, with stacks of endoplasmic reticulum, ER in close proximity. Scale bar: 5 μm. (B) RNP granule labeled in (A). The white square denotes the area of the granule in the high magnification inset. Labeling for CGH-1 tends to be localized in the more densely staining areas of the granules. Scale bar: 1 μm. (C–D) Stacks of membranes labeled for nuclear pore proteins with 12 nm gold particles, in close proximity to an unlabeled RNP granule. (C′–D′) Schematic drawings. (C) Stacks of membrane are located close to a structure with the same appearance as previously observed RNP granules labeled in (A–B). Scale bar: 1 μm. (D) High magnification of the stacked membranes in (C). Scale bar: 0.5 μm. (E–F) Costaining for CGH-1 (12 nm gold) and nuclear pore proteins (6 nm gold). (E′–F′) Schematic drawings. (E) An RNP granule next to stacked membranes. Scale bar: 1 μm. (F) High magnification image of (E). The membrane structure is labeled with 6 nm gold (white arrow) and the RNP granule components with 12 nm gold (black arrow). The white square denotes the area in the membrane structure in the high magnification inset, which better shows the labeling for nuclear pore proteins.

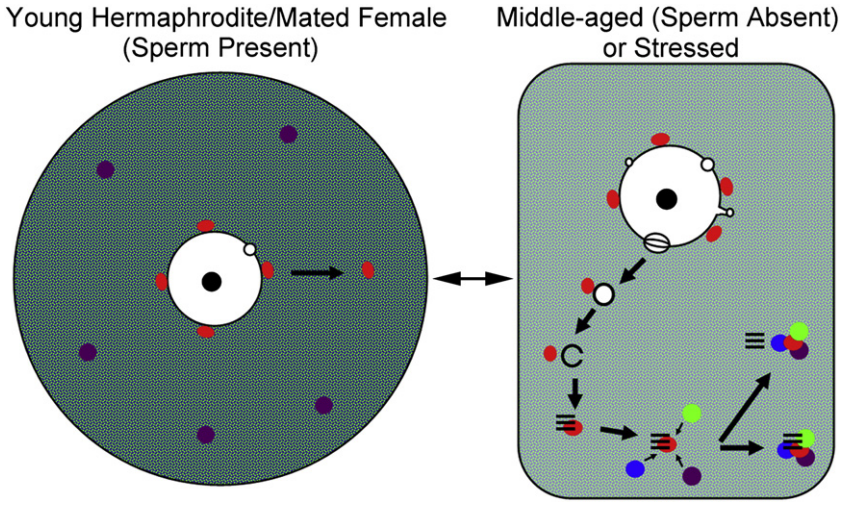

Fig. 9. Model of nucleoporin trafficking, linking nuclear membrane blebbing with the formation of annulate lamellae and assembly of RNP granules in arrested and stressed oocytes. In oocytes of young hermaphrodites or mated females when sperm is present, several RNA-binding proteins are distributed uniformly throughout the cytoplasm (green and blue), while others, such as P body proteins are found in small punctuate granules (purple). In proximal oocytes, P granules (red) detach from the nuclear membrane and become cytoplasmic. Few blebs are detected, and no large RNP granules assemble. In middle-aged worms without sperm or in stressed worms, an increase in nuclear blebbing on the nuclear envelope occurs. Nuclear blebs detach and P granules associate near the blebs in the cytoplasm (red). The spherical blebs become reorganized into stacks of annulate lamellae (parallel lines) that remain in close in proximity to P granules. The annulate lamellae-P granule complex then recruits other RNP granule components (purple is P body proteins; green and blue represent previously dispersed, RNA-binding proteins). The annulate lamellae may then dissociate from, or remain adjacent to, the large RNP granule at the cell cortex.

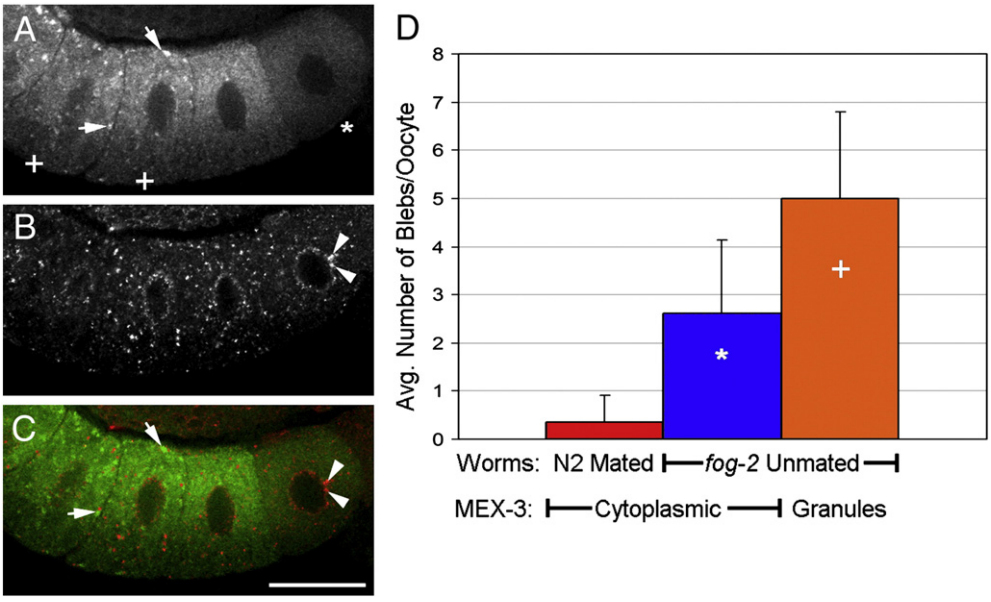

Fig. 10. Nuclear membrane blebs form before MEX-3 assembles into large granules. (A–C) Arrested oocytes from unmated *fog-2* female at 6-h post-L4. (A) MEX-3 has begun localizing into granules (arrows) in most proximal oocytes (+) but remains cytoplasmic in more distal oocytes (*). (B) Nuclear pore proteins detected with mAb414 reveal nuclear blebs in distal oocytes (arrowheads). (C) Merged image of MEX-3 and mAb414. Scale bar: 20 μm. (D) Quantitation of nuclear blebs in oocytes. Few blebs are detected in oocytes of wild-type hermaphrodites (red). Increased numbers of blebs are detected in oocytes with cytoplasmic MEX-3 (blue), i.e., prior to the assembly of granules. This is consistent with the model suggesting increased blebbing precedes RNP granule formation.

oocyte viability with increased nuclear blebbing and RNP granule assembly.

In *Drosophila* oocytes, RNP complexes of Orb, Me31b, and Trailer Hitch associate with Rtnl1, a membrane protein resident in the ER that strongly localizes to the fusome (specialized subdomain of the ER) of egg chambers. These membranes in the germline of *Drosophila* may play a role in anchoring, localizing, or transporting RNP complexes in the oocyte (Roper, 2007). Although the distribution of ER proteins in arrested or stressed oocytes was not the focus of this study, we did observe dramatic changes in the architecture of the ER in aging or stressed oocytes (Fig. 7A and C; Supplemental Table 1). The large sheets of ER may represent specialized ER/annulate lamellae that recruit RNPs to become localized to the cell cortex, similar to the idea in *Drosophila* that RNP complexes may "hitchhike" on specialized ER that appears to be actively transported into the growing oocyte (Roper, 2007). Our model speculates that portions of the nuclear membrane, a distinct domain of the continuous ER network, actively bleb into the cytoplasm, migrate to the cell cortex where they reorganize into linear, aligned membranes known as annulate lamellae, and promote the assembly of large RNP granules at the oocyte cortex (Fig. 9). To gain insight into the directionality of the nuclear membrane trafficking, we did time-lapse imaging after heat shock using a strain with a labeled nucleoporin, GFP::NPP-9 (Voronina and Seydoux, 2010). We observed at least one clear example of a portion of nuclear membrane trafficking from the nuclear envelope to the cell cortex (Supplemental Movie 1), thus

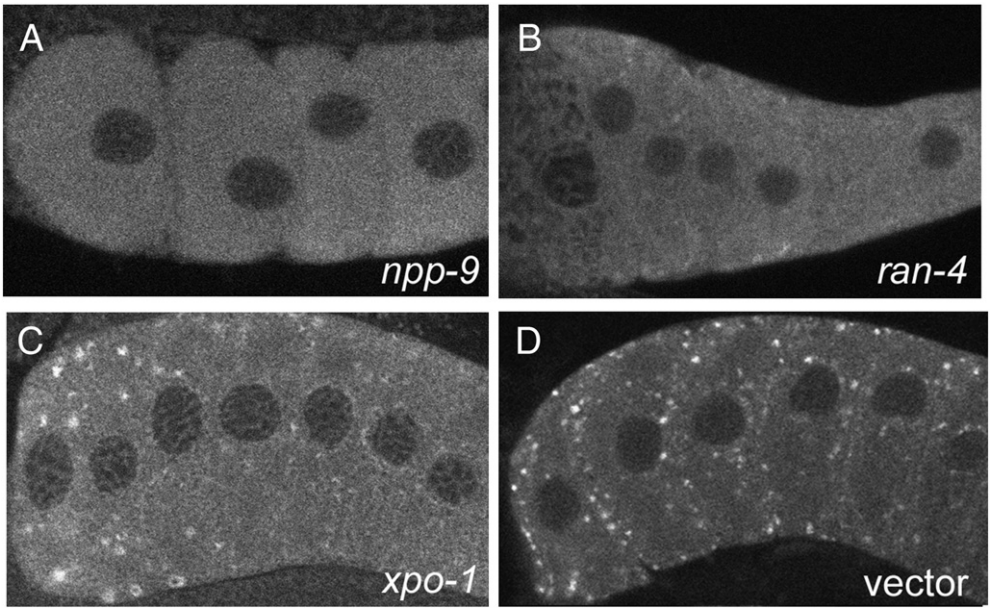

Fig. 11. Some nuclear pore complex proteins are required for the assembly of MEX-3 granules. (A–D) Detection of MEX-3 in *fog-2* unmated females after RNAi of (A) *npp-9*, (B) *ran-4*, (C) *imb-4*, (D) L4440 vector control.

discounting the likelihood that nuclear blebs represent unidirectional shuttling from the cytoplasm to the nuclear envelope. We also do not favor this latter unidirectional model because we see increased nuclear blebbing along the nuclear envelope prior to any dramatic changes in the cytoplasm (Fig. 10). Although our data do not rule out the possibility that blebs represent bidirectional trafficking, multiple lines of evidence are consistent with our current model emphasizing trafficking from the nuclear envelope to the cortex. First, we observe a large increase in both the number of nuclear blebs and large RNP granules only in arrested and stressed oocytes; their appearance is coordinated (Table 1). Second, we detect assemblies of annulate lamellae in close proximity to RNP granules in arrested and stressed oocytes (Fig. 6). Annulate lamellae represent specialized ER membranes that contain aligned nuclear pore complexes; their function is not clear, but they have been observed in oocytes of many species, and especially in cells in which there is a substantial delay between transcription and translation (Kessel, 1989). In studies of *Necturus maculosus* and *Thyone briareus* oocytes, the annulate lamellae appear to form through the fusion of detached vesicular blebs of the outer nuclear membrane (Kessel, 1963; Kessel, 1966). Third, an increased number of nuclear membrane blebs on the nuclear envelope are seen in young *fog-2* females prior to the relocalization of MEX-3 into large granules (Fig. 10). Finally, when components of nuclear pore complexes are knocked-down by RNAi, the assembly of MEX-3 into large granules is disrupted (Fig. 11).

The failure of MEX-3 granules to form after RNAi of several nucleoporins and nuclear transport receptors is intriguing. We selected these 6 genes, in part, because they regulate the proper localization of P granules in early embryos (Updike and Strome, 2009; Voronina and Seydoux, 2010). Our results, in combination with these published data, support a functional relationship between assembly and localization of germline RNP granules and NPC components. Since nucleoporins are required for multiple cellular processes, our results may be due to indirect effects of knocking down expression of the nucleoporins. XPO-1 is a nuclear export receptor required for primary miRNA processing and *xpo-1(RNAi)* phenocopies several aspects of the *let-7* heterochronic phenotype (Büssing et al., 2010). Three of the genes, *npp-9* (RanBP2), *ran-1* (Ran GTPase), and *ran-4* (nuclear transport factor 2), are members of the Ran family that regulates the transport of RanGTPase into the nucleus (Weiss, 2003). *ran-1* is a negative regulator of oocyte meiotic maturation, is localized to the oocyte cortex, and functions in the germline (Govindan et al., 2006; Cheng et al., 2008). Both *ran-1* and *npp-9* regulate microtubule dynamics in mitotic and interphase cells (Joseph and Dasso, 2008; Joseph, 2006). Since microtubules are necessary for assembly of RNP complexes such as stress granules (Ivanov et al., 2003), the requirement for *npp-9* and *ran-4* for MEX-3 granule formation in oocytes may indicate a role for microtubules in RNP assembly in meiotic cells.

One of our goals was to compare the ultrastructure of RNP granules induced by stress and extended meiotic arrest with the ultrastructure of other characterized RNPs. The categorization of the oocyte RNP granules within the various classes of RNPs has not been straightforward as they contain typical marker proteins of P granules, P bodies, and stress granules (Jud et al., 2008). Their size varies, but the largest RNP granules (3 μm in diameter) are much larger than the largest P bodies, which are approximately 300 nm in diameter in mammalian cells (Yang and Schoenberg, 2004; Souquere et al., 2009). P bodies are often seen in the cytoplasm adjacent to the nuclear envelope and have been suggested to serve as potential storage sites for newly exported mRNA, though no P bodies have yet been observed directly adjacent to well defined nuclear pore structures. One of the markers often used to identify P bodies is Rck/p54 (Souquere et al., 2009), the same protein we targeted in our immunoEM experiments to granules near the cell cortex that were much larger than P bodies (Fig. 8). Thus, it seems appropriate to conclude the large oocyte RNP granules share characteristics with P bodies, but are a distinct type of RNP. Stress granules are a larger RNP that forms in response to cellular stresses including heat shock (Kedersha and Anderson, 2007); they appear to be granular and have a distinct ultrastructure from P bodies, which are more fibrillar (Souquere et al., 2009). The fine structure of the oocyte RNP granules seemed somewhat similar to that of heat shock-induced stress granules, including the presence of dense fibrillar patches within the granules (Fig. 7A and B); however, abundant membranes as observed adjacent to large oocyte RNP granules (Fig. 7C and D) were not observed in close proximity to stress granules (Souquere et al., 2009). Differences in the ultrastructure of stress granules and oocyte RNP granules could be explained by different fixation or staining conditions or may reflect a more fundamental difference between these RNPs.

Multiple lines of evidence suggest the oocyte RNP granules induced by extended meiotic arrest or stress may be analogous to the RNP structure in *Drosophila* ovaries known as the sponge body, which was first described based on its appearance by TEM and its enrichment of RNA localization factors, such as Exuperantia and RNA (Wilsch-Brauninger et al., 1997). First, their composition is similar to the proteins localized in arrested worm oocytes, including Me31B (ortholog of CGH-1), Tral (ortholog of CAR-1), Dcp2 (ortholog of DCAP-2) (Nakamura et al., 2001; Lin et al., 2006; Jud et al., 2008; Noble et al., 2008; Wilhelm et al., 2005), and some proteins such as Staufen are compartmentalized within subdomains of the large bodies. Secondly, the architecture of sponge bodies changes in virgin females and in flies fed a diet lacking yeast, from a dispersed pattern to a reticulated distribution and to a more complex composition (Snee and Macdonald, 2009). These dynamics are similar to the changes we see in oocytes of unmated *Caenorhabditis* females where dispersed proteins such as MEX-3 and small P granules become concentrated into much larger, more complex RNP granules that are often spherical, but sometimes irregularly shaped (Jud et al., 2007, 2008; Fig. 1). Third, sponge bodies are much larger than P bodies at ~3 μm in diameter, very similar in size to the RNP granules characterized here (Fig. 7). Fourth, sponge bodies are associated with the ER (Wilsch-Brauninger et al, 1997), similar to the enrichment of membranes we observe throughout the electron dense RNPs at the oocyte cortex (Fig. 7). The link between the secretory pathway and RNP complexes was also suggested when Tral was identified as a P body component that localizes to the ER in *Drosophila* oocytes (Wilhelm et al., 2005). P bodies and sponge bodies appear to be closely related structures, and their names have at times been used interchangeably (Decker and Parker, 2006; Lin et al., 2006). Interestingly, no obvious changes were noted in the organization of the ER when reticulated sponge bodies form, at least at the light microscopy level of resolution (Snee and Macdonald, 2009), while our studies demonstrate fairly dramatic changes as large sheets of ER are visible using TEM (Fig. 7). Fifth, the presence of reticulated sponge bodies does not interfere with early embryonic development in flies, nor does the presence of RNP granules disrupt embryonic hatching in worms (Snee and Macdonald, 2009; Jud et al., 2008). Finally, at least one additional difference exists between sponge bodies and the worm oocyte RNP granules. The worm RNP granules contain high levels of both poly(A) binding protein (PABP) and TIA-1, two markers of stress granules (Jud et al., 2008). In contrast, sponge bodies lack PABP and ribosomes and therefore have been characterized as distinct from stress granules (Snee and Macdonald, 2009). The function of neither reticulated sponge bodies nor RNP granules is clear, but all evidence is consistent with these bodies having a role in mRNA storage, trafficking, or remodeling. Further studies are needed to discern the roles these dynamic RNP particles play in the germline.

The nuclear membrane has long been known to undergo dynamic remodeling during mitosis; however, fewer studies have focused on changes during meiosis (Hetzer et al., 2005). The nuclear membrane blebs in arrested and stressed oocytes described here are somewhat

reminiscent of the accessory nuclei (AN) described in hymenopteran insects (Jaglarz et al., 2008). Accessory nuclei bud from the oocyte nucleus and are surrounded by membrane identical to the nuclear envelope including the presence of nuclear pores. However, in contrast to AN that can occur by the tens or hundreds in a single oocyte, and which contain an electron dense pseudonucleolus containing snRNPs, the nuclear membrane blebs described here were observed much less frequently (Table 1), lacked a pseudonucleolus (Figs. 2 and 5), and did not stain positively for RNA (JA Schisa, unpublished results). The term "nuclear bleb" has been used to describe a number of different nuclear membrane extensions, perhaps first used to describe evaginations of the inner membrane of the nuclear envelope in the pronuclei of rat and rabbit zygotes (Szollosi, 1965; Gulyas, 1971). Nuclear blebbing has also been described in oocytes from cattle, monkeys and humans (Baker and Franchi, 1969; Szollosi and Szollosi, 1988). The nuclear membrane blebs characterized here appear to differ structurally from most, if not all, previously described nuclear membrane blebs in germ cells. For example, in tunicate oocytes, the outer nuclear membrane is described as blebbing away from the inner membrane, resulting in an increase in the diameter of the perinuclear space, but not the presence of additional membranes (Kessel, 1965). In humans similar blebs affecting either the inner or outer membrane have been described in pronucleate eggs and early embryos (Zamboni et al., 1966). The average diameter of nuclear blebs in mouse zygotes is approximately 10-fold less than the blebs observed here (Szollosi and Szollosi, 1988; Table 1). Thus, no previously described nuclear blebs share both similar size and morphology characteristics with those described here. One reason these types of nuclear blebs have not been previously described may be that they are unique to the physiological conditions of being stressed or in extended meiotic arrest. It will be interesting in future studies to see if heat stress or extended meiotic arrest, as occurs in oocytes of aging mammalian females, induces similar nuclear blebs in organisms in addition to the two species of *Caenorhabditis* described here. Our studies indicate a new role for nuclear membrane blebs, as a transition state of nucleoporin shuttling to the cell cortex, that we speculate is required for the assembly of large RNP granules and ultimately functions to help preserve oocyte viability when fertilization is delayed.

Supplementary materials related to this article can be found online at doi:10.1016/j.ydbio.2011.02.028.

Acknowledgments

We gratefully acknowledge the generosity of David Hall and Ken Nguyen at Albert Einstein College of Medicine for extensive training in immunoEM methods. We acknowledge Emily Petty for the preliminary results with *kgb-1*. We thank Jim Priess (Fred Hutchinson Cancer Research Center), Susan Strome (UC Santa Cruz), and David Greenstein (University of Minnesota) for antibodies, Gyorgyi Csankovski (University of Michigan) for RNAi clones, Ekaterina Voronina and Geraldine Seydoux (Johns Hopkins University School of Medicine) for the GFP::NPP-9 strain, and Phil Oshel in the CMU Microscopy Facility for TEM and confocal microscopy advice. This work was supported by the National Institutes of Health grants 1R15GM078157-01, 1R15GM093913-01, and National Science Foundation grant MRI 0923155 to J.A.S.

References

Anderson, P., Kedersha, N., 2006. RNA granules. J. Cell Biol. 172, 803–808.
Aris, J.P., Blobel, G., 1989. Yeast nuclear envelope proteins cross react with an antibody against mammalian pore complex proteins. J. Cell Biol. 108, 2059–2067.
Baker, T.G., Franchi, L.L., 1969. The origin of cytoplasmic inclusions from the nuclear envelope of mammalian oocytes. Z. Zellforsch. Mikrosk. Anat. 93, 45–55.
Blower, M.D., et al., 2005. A Rae1-containing ribonucleoprotein complex is required for mitotic spindle assembly. Cell 121, 223–234.
Brenner, S., 1974. The genetics of Caenorhabditis elegans. Genetics 77, 71–94.
Browning, H., Strome, S., 1996. A sperm-supplied factor required for embryogenesis in C. elegans. Development 122, 391–404.
Buchan, J.R., Nissan, T., Parker, R., 2010. Analyzing P-bodies and stress granules in Saccharomyces cerevisiae. Methods Enzymol. 470, 619–640.
Büssing, I., Yang, J.S., Lai, E.C., Grosshans, H., 2010. The nuclear export receptor XPO-1 supports primary miRNA processing in *C. elegans* and *Drosophila*. EMBO J. 29, 1830–1839.
Cheng, H., Govindan, J.A., Greenstein, D., 2008. Regulated trafficking of the MSP/Eph receptor during oocyte meiotic maturation in *C. elegans*. Curr. Biol. 18, 705–714.
Decker, C.J., Parker, R., 2006. CAR-1 and trailer hitch: driving mRNP granule function at the ER? J. Cell Biol. 173, 159–163.
Draper, B.W., Mello, C.C., Bowerman, B., Hardin, J., Priess, J.R., 1996. MEX-3 is a KH domain protein that regulates blastomere identity in early C. elegans embryos. Cell 87, 205–216.
Govindan, J.A., Cheng, H., Harris, J.E., Greenstein, J.E., 2006. Galphao/i and Galphas signaling function in parallel with the MSP/Eph receptor to control meiotic diapause in C. elegans. Curr. Biol. 16, 1257–1268.
Gulyas, B.J., 1971. The rabbit zygote: formation of annulate lamellae. J. Ultrastruct. Res. 35, 112–126.
Hajeri, V.A., Little, B.A., Ladage, M.L., Padilla, P.A., 2010. NPP-16/Nup50 function and CDK-1 inactivation are associated with anoxia-induced prophase arrest in *Caenorhabditis elegans*. Mol. Biol. Cell 21, 712–724.
Hall, D.H., Hartweig, E., Nguyen, K.C.Q., 2011. Modern electron microscopy methods for *C. elegans*. In: Rothman, Joel (Ed.), Methods in Cell Biology. Academic Press, New York.
Hetzer, M.W., Walther, T.C., Mattaj, I.W., 2005. Pushing the envelope: structure, function, and dynamics of the nuclear periphery. Annu. Rev. Cell Dev. Biol. 21, 347–380.
Ivanov, P.A., Chudinova, E.M., Nadezhdina, E.S., 2003. Disruption of microtubules inhibits cytoplasmic ribonucleoprotein stress granule formation. Exp. Cell Res. 290, 227–233.
Jaglarz, M.K., Kloc, M., Bilinski, S.M., 2008. Accessory nuclei in insect oogenesis: in search of the function of enigmatic organelles. Int. J. Dev. Biol. 52, 179–185.
Joseph, J., 2006. Ran at a glance. J. Cell Sci. 119, 3481–3484.
Joseph, J., Dasso, M., 2008. The nucleoporin Nup358 associates with and regulates interphase microtubules. FEBS Lett. 582, 190–196.
Jud, M., Razelun, J., Bickel, J., Czerwinski, M., Schisa, J.A., 2007. Conservation of large foci formation in arrested oocytes of Caenorhabditis nematodes. Dev. Genes Evol. 217, 221–226.
Jud, M.C., Czerwinski, M.J., Wood, M.P., Young, R.A., Gallo, C.M., Bickel, J.S., Petty, E.L., Mason, J.M., Little, B.A., Padilla, P.A., Schisa, J.A., 2008. Large P body-like RNPs form in C. elegans oocytes in response to arrested ovulation, heat shock, osmotic stress, and anoxia and are regulated by the major sperm protein pathway. Dev. Biol. 318, 38–51.
Kamath, R.S., Ahringer, J., 2003. Genome-wide RNAi screening in Caenorhabditis elegans. Methods 30, 313–321.
Kedersha, N., Anderson, P., 2007. Mammalian stress granules and processing bodies. Methods Enzymol. 431, 61–81.
Kedersha, N., Stoecklin, G., Ayodele, M., Yacono, P., Lykke-Andersen, J., Fritzler, M.J., Scheuner, D., Kaufman, R.J., Golan, D.E., Anderson, P., 2005. Stress granules and processing bodies are dynamically linked sites of mRNP remodeling. J. Cell Biol. 169, 871–884.
Kessel, R.G., 1963. Electron microscope studies on the origin of annulate lamellae in oocytes of necturus. J. Cell Biol. 19, 391–414.
Kessel, R.G., 1965. Intranuclear and cytoplasmic annulate lamellae in tunicate oocytes. J. Cell Biol. 24, 471–487.
Kessel, R.G., 1966. Some observations on the ultrastructure of the oocyte of Thyone briareus with special reference to the relationship of the Golgi complex and endoplasmic reticulum in the formation of yolk. J. Ultrastruct. Res. 16, 305–319.
Kessel, R.G., 1989. The annulate lamellae—from obscurity to spotlight. Electron Microsc. Rev. 2, 257–348.
Kiontke, K., Fitch, D.H.A., 2005. The phyologenetic relationships of *Caenorhabditis* and other rhabditids (August 11, 2005), WormBook, ed. The *C. elegans* Research Community, WormBook, doi/10.1895/wormbook.1.11.1, http://www.wormbook.org.
Lin, M.D., Fan, S.J., Hsu, W.S., Chou, T.B., 2006. Drosophila decapping protein 1, dDcp1, is a component of the oskar mRNP complex and directs its posterior localization in the oocyte. Dev. Cell 10, 601–613.
Lucocq, J., 2008. Quantification of structures and gold labeling in transmission electron microscopy. Methods Cell Biol. 88, 59–82.
Luo, S., Kleemann, G.A., Ashraf, J.M., Shaw, W.M., Murphy, C.T., 2010. TGF-beta and insulin signaling regulate reproductive aging via oocyte and germline quality maintenance. Cell 143, 299–312.
McCarter, J., Bartlett, B., Dang, T., Schedl, T., 1999. On the control of oocyte meiotic maturation and ovulation in Caenorhabditis elegans. Dev. Biol. 205, 111–128.
Nakamura, A., Amikura, R., Hanyu, K., Kobayashi, S., 2001. Me31B silences translation of oocyte-localizing RNAs through the formation of cytoplasmic RNP complex during Drosophila oogenesis. Development 128, 3233–3242.
Navarro, R.E., Shim, E.Y., Kohara, Y., Singson, A., Blackwell, T.K., 2001. cgh-1, a conserved predicted RNA helicase required for gametogenesis and protection from physiological germline apoptosis in C. elegans. Development 128, 3221–3232.
Noble, S.L., Allen, B.L., Goh, L.K., Nordick, K., Evans, T.C., 2008. Maternal mRNAs are regulated by diverse P body-related mRNP granules during early Caenorhabditis elegans development. J. Cell Biol. 182, 559–572.
Parker, R., Sheth, U., 2007. P bodies and the control of mRNA translation and degradation. Mol. Cell 25, 635–646.
Paupard, M.C., Miller, A., Grant, B., Hirsh, D., Hall, D.H., 2001. Immuno-EM localization of GFP-tagged yolk proteins in C. elegans using microwave fixation. J. Histochem. Cytochem. 49, 949–956.

Pitt, J.N., Schisa, J.A., Priess, J.R., 2000. P granules in the germ cells of Caenorhabditis elegans adults are associated with clusters of nuclear pores and contain RNA. Dev. Biol. 219, 315–333.
Radu, A., Moore, M.S., Blobel, G., 1995. The peptide repeat domain of nucleoporin Nup98 functions as a docking site in transport across the nuclear pore complex. Cell 81, 215–222.
Roper, K., 2007. Rtnl1 is enriched in a specialized germline ER that associates with ribonucleoprotein granule components. J. Cell Sci. 120, 1081–1092.
Schedl, T., Kimble, J., 1988. fog-2, a germ-line-specific sex determination gene required for hermaphrodite spermatogenesis in Caenorhabditis elegans. Genetics 119, 43–61.
Schisa, J.A., Pitt, J.N., Priess, J.R., 2001. Analysis of RNA associated with P granules in germ cells of C. elegans adults. Development 128, 1287–1298.
Sheth, U., Pitt, J., Dennis, S., Priess, J.R., 2010. Perinuclear P granules are the principal sites of mRNA export in adult C. elegans germ cells. Development 137, 1305–1314.
Snee, M.J., Macdonald, P.M., 2009. Dynamic organization and plasticity of sponge bodies. Dev. Dyn. 238, 918–930.
Souquere, S., Mollet, S., Kress, M., Dautry, F., Pierron, G., Weil, D., 2009. Unravelling the ultrastructure of stress granules and associated P-bodies in human cells. J. Cell Sci. 122, 3619–3626.
Strome, S., Wood, W.B., 1982. Immunofluorescence visualization of germ-line-specific cytoplasmic granules in embryos, larvae, and adults of Caenorhabditis elegans. Proc. Natl Acad. Sci. USA 79, 1558–1562.
Szollosi, D., 1965. Extrusion of nucleoli from pronuclei of the rat. J. Cell Biol. 25, 545–562.
Szollosi, M.S., Szollosi, D., 1988. 'Blebbing' of the nuclear envelope of mouse zygotes, early embryos and hybrid cells. J. Cell Sci. 91 (Pt 2), 257–267.
Updike, D.L., Strome, S., 2009. A genomewide RNAi screen for genes that affect the stability, distribution and function of P granules in Caenorhabditis elegans. Genetics 183, 1397–1419.
Voronina, E., Seydoux, G., 2010. The C. elegans homolog of nucleoporin Nup98 is required for the integrity and function of germline P granules. Development 137, 1441–1450.
Weis, K., 2003. Regulating access to the genome: Nucleocytoplasmic transport throughout the cell cycle. Cell 112, 441–451.
Wilhelm, J.E., Buszczak, M., Sayles, S., 2005. Efficient protein trafficking requires trailer hitch, a component of a ribonucleoprotein complex localized to the ER in Drosophila. Dev. Cell 9, 675–685.
Wilsch-Brauninger, M., Schwarz, H., Nusslein-Volhard, C., 1997. A sponge-like structure involved in the association and transport of maternal products during Drosophila oogenesis. J. Cell Biol. 139, 817–829.
Yang, F., Schoenberg, D.R., 2004. Endonuclease-mediated mRNA decay involves the selective targeting of PMR1 to polyribosome-bound substrate mRNA. Mol. Cell 14, 435–445.
Zamboni, L., Mishell Jr., D.R., Bell, J.H., Baca, M., 1966. Fine structure of the human ovum in the pronuclear stage. J. Cell Biol. 30, 579–600.